FABRICATION AND CHARACTERIZATION OF DYE-SENSITIZED SOLAR CELLS MODULE BASED ON NOVEL ORGANIC DYES

PONGSATHORN TONGKASEE

A THESIS SUBMITTED IN PARTIAL FULFILLMENT OF THE REQUIREMENTS
FOR THE DEGREE OF DOCTOR OF PHILOSOPHY
MAJOR IN CHEMISTRY
FACULTY OF SCIENCE
UBON RATCHATHANI UNIVERSITY
YEAR 2013

UBON RATCHATHANI UNIVERSITY

THESIS APPROVAL

DOCTOR OF PHILOSOPHY

MAJOR IN CHEMISTRY FACULTY OF SCIENCE

TITLE FABRICATION AND CHARACTERIZATION OF DYE-SENSITIZED SOLAR CELLS MODULE BASED ON NOVEL ORGANIC DYES

AUTHOR MR. PONGSATHORN TONGKASEE

EXAMINATION COMMITTEE

ASSOC. PROF. DR. VINICH PROMARAK	CHAIRPERSON
ASST. PROF. DR. TAWEESAK SUDYOADSUK	MEMBER
ASST. PROF. DR. SIRIPORN JUNGSUTTIWONG	MEMBER
DR. TINNAGON KEAWIN	MEMBER

ADVISOR T. Sudyoadsuk

(ASST. PROF. DR. TAWEESAK SUDYOADSUK)

Utith Inprasit

(ASSOC. PROF. DR. UTITH INPRASIT)

DEAN, FACULTY OF SCIENCE

H. Juthamas.

(DR. JUTHAMAS HONGTHONG)

ACTING FOR VICE PRESIDENT

FOR ACADEMIC AFFAIRS

ACADEMIC YEAR 2013

ACKNOWLEDGMENTS

I would like to acknowledge my advisor, Asst.Prof.Dr.Taweesak Sudyoadsuk who set the instruments for the device measurement, for his guidance on the DSSCs fabrication and for everything in this work and I wish to thank Asst.Prof.Dr.Siriporn Jungsuttiwong and Dr.Tinnagon Keawin for constructive comments and suggestion, in particular, Assoc.Prof.Dr.Vinich Promarak for his guidance on the DSSCs knowledge.

I would like to thank Ms.Duangratchaneekorn Muenmart, Ms.A-monrat Thangthong for synthesis of newly organic dyes used in this work. I am very thankful to thank Department of Physics and, Department of Bioscience, Faculty of Science Ubon Ratchathani University for XRD and SEM measurement, respectively.

Moreover, I am also thankful to Center of Excellent for Innovation in Chemistry (PERCH-CIC), Precise Green Technology and Service CO., Ltd for the scholarship and Department of Chemistry Faculty of Science Ubon Ratchathani University for financial support. Finally, I am deeply grateful to my family for their love, support, and encouragement.

Pongsathorn Tongkasee

Researcher

บทคัดย่อ

ชื่อเรื่อง : การสร้างและการศึกษาเซลล์แสงอาทิตย์ชนิดสีย้อมไวแสง
แบบโมดูลด้วยสีย้อมไวแสงสารอินทรีย์ชนิดใหม่

โดย : พงศธร ทองกระสี

ชื่อปริญญา : ปรัชญาดุษฎีบัณฑิต

สาขาวิชา : เคมี

ประธานกรรมการที่ปรึกษา : ผู้ช่วยศาสตราจารย์ ดร.ทวีศักดิ์ สุดยอดสุข

ศัพท์สำคัญ : เซลล์แสงอาทิตย์ชนิดสีย้อมไวแสง กระบวนการขึ้นรูปแบบปริ้นสกรีน สีย้อมไวแสงชนิดสารอินทรีย์

เซลล์แสงอาทิตย์ชนิดสีย้อมไวแสงได้รับความสนใจอย่างมากเนื่องจากมีราคาถูกและกระบวนการเตรียมที่ไม่ยุ่งยาก งานวิจัยนี้ทำการขึ้นรูปและพัฒนาเซลล์แสงอาทิตย์ชนิดสีย้อมไวแสงโดยกระบวนการขึ้นรูปอย่างง่ายแบบปริ้นสกรีน ประสิทธิภาพของเซลล์แสงอาทิตย์ชนิดสีย้อมไวแสงสามารถปรับปรุงให้เพิ่มขึ้นได้โดยใช้ไลหะออกไซด์ไทเทเนียมที่เหมาะสมและจำนวนชั้นของฟิล์มบางของไทเทเนียมที่พอเหมาะ โดยส่งผลต่อปริมาณของสีย้อมที่ยึดเกาะบนไทเทเนียมไดออกไซด์ และผลของแรงต้านทาน สีย้อมสารอินทรีย์ชนิดใหม่เป็นตัวเลือกหนึ่งที่นำมาใช้ประโยชน์ในเซลล์แสงอาทิตย์ชนิดสีย้อมไวแสง เนื่องจากสังเคราะห์ได้ง่าย ราคาถูก ไม่เป็นพิษ และออกแบบโมเลกุลได้ง่าย จากการศึกษาแสดงให้เห็นถึงการนำเอาสีย้อมไวแสงชนิดสารอินทรีย์ชนิดใหม่มาใช้ทดสอบกับเซลล์ทดลองและประยุกต์ใช้กับเซลล์ต้นแบบ การปรับปรุงประสิทธิภาพเซลล์แสงอาทิตย์ชนิดสีย้อมไวแสงอย่างหนึ่ง คือการปรับปรุงการดูดกลืนแสงหรือ การปรับเปลี่ยนองค์ประกอบทางเคมีที่เหมาะสมของสารอิเล็กโทรไลต์ โดยช่วยเพิ่มประสิทธิภาพในการเปลี่ยนพลังงานแสงอาทิตย์เป็นกระแสไฟฟ้า กระบวนการขึ้นรูปและสารอินทรีย์ชนิดใหม่เหล่านี้เป็นทางเลือกหนึ่งในการพัฒนาเซลล์แสงอาทิตย์ชนิดสีย้อมไวแสงชนิดสารอินทรีย์แบบโมดูลต้นทุนต่ำ

ABSTRACT

TITLE : FABRICATION AND CHARACTERIZATION OF DYE-SENSITIZED SOLAR CELL MODULE BASED ON NOVEL ORGANIC DYES

BY : PONGSATHORN TONGKASEE

DEGREE : DOCTOR OF PHILOSOPHY

MAJOR : CHEMISTRY

CHAIR : ASST.PROF.TAWEESAK SUDYOADSUK, Ph.D.

KEYWORDS : DYE-SENSITIZED SOLAR CELLS / SCREEN-PRINTING PROCESS / ORGANIC SENSITIZER

Dye-sensitized solar cells (DSSCs) have aroused intense interest over the past decade owing to their low cost and simple preparation procedure. The screen-printing technique is the simple procedure for preparation and improvement of the DSSCs performance. The efficiency of DSSCs device could be improved by using the suitable TiO_2 paste and enough amount of TiO_2 layer. The amount of TiO_2 layers were affected to the quantity of dye absorption and device resistivity. The novel organic dye is a choice of sensitizer as application in DSSCs performance due to the advantage of simple synthesized, low cost, non toxicity and easy molecular designed. The studies show the operation of organic sensitizer in DSSCs test cells and applied to prototype cells. The improvement of DSSCs operation by modifying the light absorbing or much easier approach, optimization of the electrolyte component would also lead to increased device efficiency. These procedure and novel synthesized materials could be alternative for development of low cost DSSCs module.

CONTENTS

CONTENTS (CONTINUED)

LIST OF TABLES

LIST OF FIGURES

LIST OF FIGURES (CONTINUED)

LIST OF FIGURES (CONTINUED)

LIST OF FIGURES (CONTINUED)

LIST OF FIGURES (CONTINUED)

LIST OF ABBREVIATIONS

ABBREVIATION	DEFINITION
HOMO	Highest occupied molecular orbital
LUMO	Lowest unoccupied molecular orbital
DSSCs	Dye-sensitized solar cells
W	Watt
AM	Air mass
nm	Nano metre
V_{oc}	Open circuit voltage
I_{sc}	Short-circuit current
FF	Fill factor
η	Conversion efficiency
IPCE	Incident Photon to Current Conversion Efficiency
eV	Electron volt
A	Ampere
dm^2	Square decimeter
AFM	Atomic force microscopy
ITO	Indium tin oxide
wt%	Weight percentage
D-π-A	Donor-π-acceptor
ILs	Ionic liquids
RTIL	Room temperature ionic liquid
cP	Centi point
CE	Counter electrode
R_{CT}	Charge transfer resistance
Ω	Ohm
cm	Centimeter
FTO	Fluorine-doped tin oxide
μm	Micrometer

LIST OF ABBREVIATIONS (CONTINUED)

ABBREVIATION	DEFINITION
m	Meter
mm	Millimeter
μm	Micrometer
λ	Wavelength of the incident light
LHE	Light harvesting efficiency
η_{reg}	Dye regeneration efficiency
η_{cc}	Charge collection efficiency
J	Jules
E_{CB}	Energy level of conduction band
λ_{max}	Wavelength maximum
ε	Molar extinction coefficient
τ	Electron life times
ICT	Intramolecular charge-transfer transition
'C	Celsius degree
I	Current
J	Current density
V	Voltage
mL	Milliliter
%	Percent
s	Second
M	Molarity
L	Liter
m/n	Minute
UV	Ultra-violet
EQE	External Quantum Efficiency
p	Pico

CHAPTER 1

INTRODUCTION

1.1 Introduction

The primary energy was used in the twentieth century as fossil fuels. Between 1980 and 2006, the world's wide annual growth rate was 2%. The fossil fuel was supplied for the world energy as 86%. From 1965 to 2008, the use of fossil fuels has continued to grow and their share of the energy supply has increased. From 2003 to 2008, coal, which is one of the dirtiest sources of energy, was the fastest growing fossil fuel. In 2005 nuclear power accounted for 6.3% of world's total primary energy supply. The nuclear power production in 2006 accounted for 16% of world's total electricity production. The development of nuclear power in the world essential was stopped with Chernobyl, but has been revisited in 2009 because of concerns of global warming from using fossil fuels, and then in 2011, the Fukushima Daiichi nuclear disaster is the second disaster to measure Level 7 on the International Nuclear Event Scale, releasing an estimated 10 to 30% of the radiation of the Chernobyl accident [1]. Therefore, the wind power and solar power have emerged as the fastest growing energy sources, and the most likely replacement for fossil fuels [2].

Therefore, energy development is the progressing effort to give sufficient primary energy sources and secondary energy forms to power the world economy. It involves both installation of established technologies and research and development to creation a new energy-related technologies. Major considerations in energy planning include cost, impact on air pollution, and whether or not the source is renewable. Primary energy sources are substances or processes with concentrations of energy at a high enough potential to be feasibly encouraged to convert to lower energy forms under human control for human benefit. Except for nuclear fuels, tidal energy and geothermal energy, all terrestrial energy sources are from current solar or from fossil remains of plant and animal life that relied directly and indirectly upon sunlight, respectively.

Renewable energy is generated from natural resources-such as sunlight, wind, rain, tides and geothermal heat-which are renewable (naturally replenished). Renewable energy technologies included solar power, wind power, hydroelectricity, micro hydro, biomass and biofuels. In 2006, about 18% of global final energy consumption came from renewable energy, with 13% coming from traditional biomass, such as wood-burning.

Hydropower was the next largest renewable source, providing 3%, followed by hot water/heating, which contributed 1.3%. Modern technologies, such as geothermal, wind, solar, and ocean energy together provided some 0.8% of final energy consumption.

The renewable resources are available each year, unlike non-renewable resources which are eventually comparison is a coal mine and a forest, while the forest could be depleted, if it is managed properly continuous supply of energy ,versus the coal mine which once it has been exhausted is gone. The most of earth's available energy resources are renewable resources. Renewable resources account for more than 93% of total U.S. energy reserves. Annuals renewable resources were multiplied times thirty years for comparison with non-renewable resources. In other words, if all non-renewable sources were uniformly exhausted in 30 years, they would only account for 7% of available resource each year, if all available renewable resources were developed [3].

Most of the world's energy resources are from the sun's rays hitting earth. Some of that energy has been preserved as fossil, which is directly or indirectly usable, for example, via wind, hydro-or wave power. The estimates of remaining non-renewable worldwide energy resources vary, with the remaining fossil fuels totaling an estimated $0.4x10^{24}$ J and the available nuclear fuel such as uranium exceeding $2.5x10^{24}$ J. Fossil fuels range from $0.6x10^{24}$ to $3x10^{24}$ J, if estimation of reserve of methane is accurate and become technically extractable. Mostly thanks to the Sun, the world also has a renewable usable energy flux that exceeds 8,000 times total usage of all non-renewable resources [4].

Therefore, the solar energy was selected for world's energy supported. Solar energy can be converted directly into other forms of energy, such as heat and electricity. The major disadvantages of solar energy are:

(1) The inability to control or predict how much solar energy arrives on the earth's surface at any place.

(2) The technology to date requires that a large surface is required for collection of useful amounts of solar energy.

The strength of the solar energy available at any point on the earth depends, on the day of the year, the time of day, and the latitude of the collection point. The amount of energy collected can be further changed depending on the orientation and shape of the object doing the collection, which is a measurement of the amount of solar energy that reaches the surface of the earth. The amount of solar energy an area received was depended on the Sun's angle, the amount of dust and water steam in the air, and the amount of cloud cover. Less than half of the radiation energy we receive from the sun makes it to the ground. The rest is absorbed by the atmosphere or reflected back out into space as show in Figure 1.1.

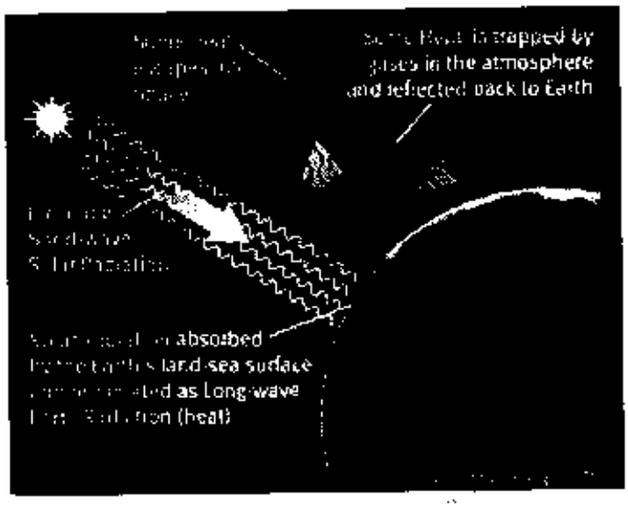

Figure 1.1 The irradiation of sunlight on the world [4].

In fact, several of the alternative energy sources used today was indirectly derived from solar energy [5]. The sun provides the earth with approximately 100,000 TW, which is almost 10,000 times more than the current energy consumption. This abundance of energy makes solar cells very attractive for electricity production.

Therefore, the first device was produced solar energy to electrical energy as solar cell [6]. The Solar cell or photovoltaic cell is a device that converts light energy to electrical energy by photovoltaic effect. Photovoltaic is the field technology and research related to the application of

solar cells as solar energy. Sometimes the term solar cell is reversed for device intended specially to capture energy from sunlight, while the term photovoltaic cell is used when the source is unspecified. Solar cell has many applications. Individual cells are used for powering small devices such as electronics calculators. The types of solar cell as show in Figure 1.2:

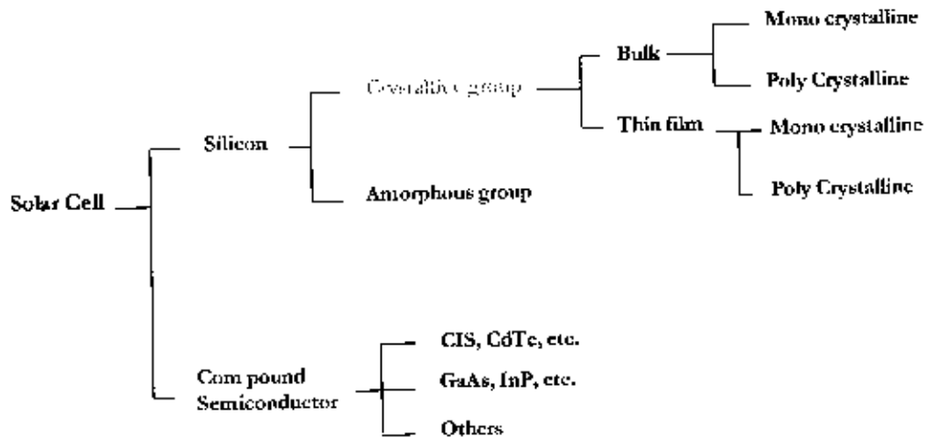

Figure 1.2 The types of solar cell.

The advent of the space program, photovoltaic cells made from semiconductor-grade silicon quickly became the power source of choice for use on satellites. The common solar power conversion efficiencies are between 15 to 20% [7]. However, the relatively high cost of manufacturing these silicon cells has been prevented their widespread use. Another disadvantage of silicon cells, were used of toxic chemicals on their manufacture. These aspects prompted the search for environmental friendly and low cost solar cell alternatives [8].

Even if the efficiency since then has increased and the production cost decreased, it is still too expensive to be unable to compete with the conventional energy sources. This has lead to a great research interest in finding new ways of utilizing the solar energy with cheaper and more efficient methods.

Since the 1950s, several new types of solar cells have been studied and developed. Among them, the dye sensitized solar cell (DSSCs). The DSSCs is a very attractive choice for utilizing the solar energy, due to its potentially low production cost. In contrast to conventional systems, where the semiconductor works as both the light absorber and charge carrier, the DSSCs separate the two functions which facilitate the production of the device. Other advantages with

DSSCs are flexibility, short energy payback time and relatively high performance at diffuse light conditions [9].

A schematic presentation of the structure and working principle of a DSSC were given in Figure 1.3. A typical, DSSCs is composed of two sheets of glass coated with a transparent conductive oxide layer. One of the glass plates (the working electrode) is covered with a film of small dye-sensitized semiconductor particles; the large surface area of the nanoparticles, which is much as a factor of 1,000 greater than the geometric area of the film, allows a monolayer of surface bound dye to absorb neatly all of the incident sunlight in the region of the spectrum where the dye absorbs. The other glass plate (the counter electrode, CE) is coated with a catalyst. From Figure 1.3, on illumination, the dye molecule absorbs photons of wavelength corresponding to the energy difference between its highest occupied molecular orbital (HOMO) and lowest unoccupied molecular orbital (LUMO) (step 1). Electrons from the ground electronic state of the dye are now promoted to excited state, known as photoexcitation of dye. This electron in the excited state of the dye is then injected into conduction band (CB) of TiO_2 (step 2). The electrons after being injected in to the CB of TiO_2 are transported through the semiconductor layer by diffusion to reach the conducting layer (step 4), FTO on glass substrate. The iodide ion now donates electron to the oxidized dye at anode and regenerates the dye molecule (step 3). The oxidized species of the electrolyte, i.e. triiodide in the iodide-triiodide complex, is reduced to iodide at the cathode (step 5). The above processes go in cycle and consequently current flows through the external circuit as long as light is incident on the cell (step 6).

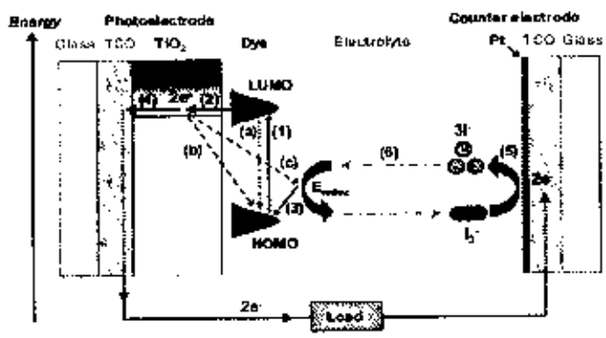

Figure 1.3 Schematic of a DSSCs structure [10].

Two electrodes are sandwiched together and the electrolyte, typically containing the iodide/triiodide (I^-/I_3^-) redox couple in an organic solvent, fills the gap between them. The basic sequence of events in the DSSCs is as follows:

Activation:

$$TiO_2/Dye \longrightarrow TiO_2/Dye^*$$

Electron injection:

$$TiO_2/Dye^* \longrightarrow TiO_2/Dye^+ + e^-(TiO_2)$$

$$e^-(TiO_2) \longrightarrow e^-(SnO_2{:}F)$$

Electron reception:

$$I_3^- + 2e^-(Pt) \longrightarrow 3I^-$$

Interception reaction:

$$3/2\ I^- + TiO_2/Dye^* \longrightarrow 1/2\ I_3^- + TiO_2/Dye$$

Upon absorption of light, an electron is injected from a metal-to-ligand charge transfer excited state of the dye into the conduction band of the metal oxide. The rate of this electron injection reaction is ultrafast, typically occurring on the order of hundreds of femtoseconds to tens of picoseconds. The injected electron percolates through the TiO_2 film, and is thought to move by a "hopping mechanism" and is driven by a chemical diffusion gradient (rather than an electric field), and is collected at a transparent conductive substrate of fluorine dope tin oxide glass (SnO_2:F), on which the TiO_2 film is printed. After passing through an external circuit, the electron is reintroduced into the solar cell at the platinum counter electrode, where triiodide is reduced to iodide. The iodide then regenerates the oxidized dye, thereby completing the circuit with no net chemical change [10-12].

The solar cell is a solid electrical device that converts solar energy directly to electricity. There are two fundamental of functions of solar cells: photo-generation of charge carriers (electrons and holes) in a light-absorbing material and separation of the charge carries to a conductive interaction to transmit electricity, adding to the wide range of solar cells, hybrid solar cells based on inorganic and organic compounds are a promising renewable energy source.

The solar cell system developed in this project is DSSCs, composed of the TiO_2 layer acting as the electron carrier and the organic dye layer acting as the electron generation, which will recover to its original state by electron donated by the electrolyte solution. The efficiency of solar cells is one of the greatest limiting factors for solar cells. In order to become an efficient solar cell, the photo sensitizer, which is the organic dye layer mentioned above must have characteristics corresponding to the spectrum of available light. Different photo sensitizers will have different absorption of available light, thus a different efficiency and cost.

Much research has been devoted to device fabrication and material development. In terms of the device fabrication process, the device operation can be improved by adsorption the dye molecule uniformly with the whole negative electrode material, which facilitated the great enhancement of adsorption capacity for molecule [13-16], designed and synthesized dye molecule for use as sensitizers [17-21], alternated electrolyte system [22, 23] and improved counter electrode system [24].

The preparation of DSSCs, the suitable for preparing TiO_2 film are doctor-blade technique, screen-printing and spin coating [25-27]. Techniques for TiO_2 film preparation will had a great advantage because this is convenient and allows large-scale manufacturing. In DSSCs, the sensitizer is one of the key components for high power-conversion efficiency. In recent years, much interest in metal-free organic dyes as an alternative to noble metal complexes has increased due to many advantages, such as diversity of molecular structures, high molar extinction coefficient, simple synthesis as well as low cost and environmental issues. The requirements of sensitizer should be good photo response in the visible region, high long-term stability under sun soaking, and appropriate HOMO and LUMO levels matching the redox potential of electrolyte and the conduction band of TiO_2 [28, 29].

So far, the commercialization has mostly reached prototypes of solar cell modules, materials and components for the building and study of small scale cells.

Here we have developed the new materials, recently, t-Butyl carbazole-alkyl-carbazole derivatives based dye as shown in Figure 1.4, Carbazole-dendron derivatives (G-series) based dye as shown in Figure 1.5 and t-Butyl carbazole-phenothiazine derivatives based dye as shown in Figure 1.6. Up to now, the development of large size DSSCs modules based on novel organic dye, which has restricted the wide practical use of this type solar cells. The novel dyes had been

designed and synthesized by our group. We hoped that these materials will be high efficient sensitizer for DSSCs.

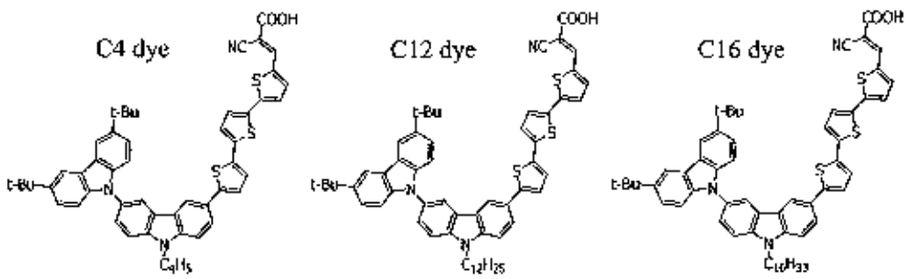

Figure 1.4 t-Butyl carbazole-alkyl-carbazole derivatives based dye (C-series).

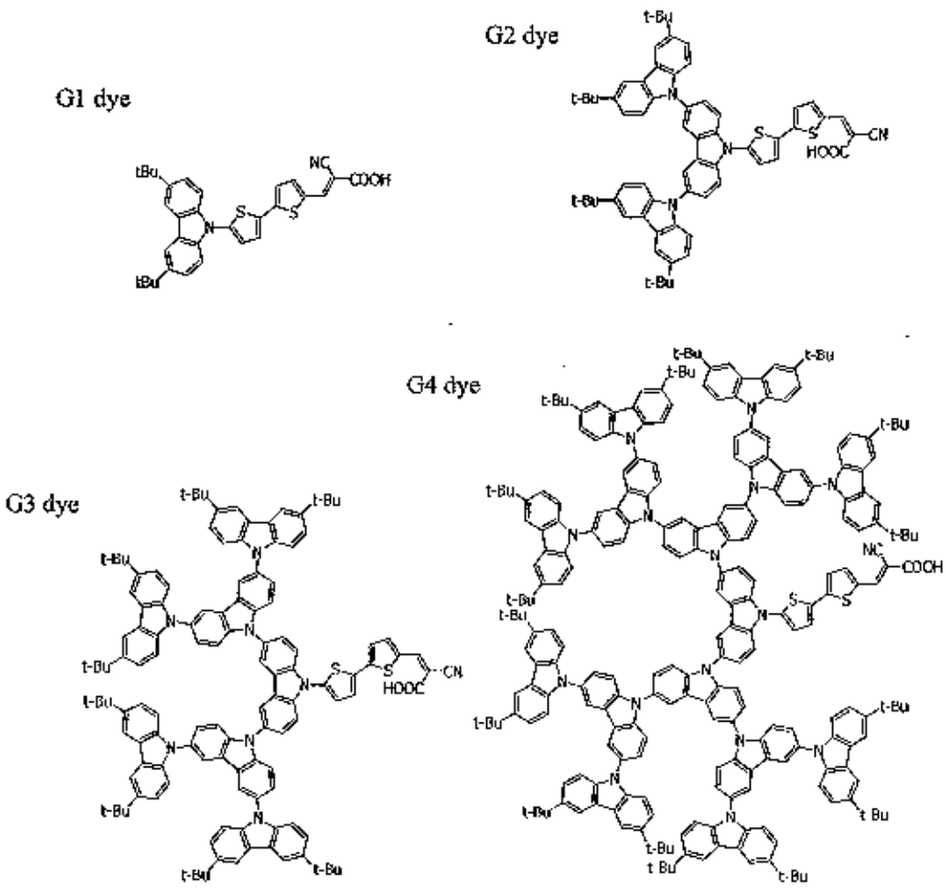

Figure 1.5 Carbazole-dendron derivatives base dye (G-series).

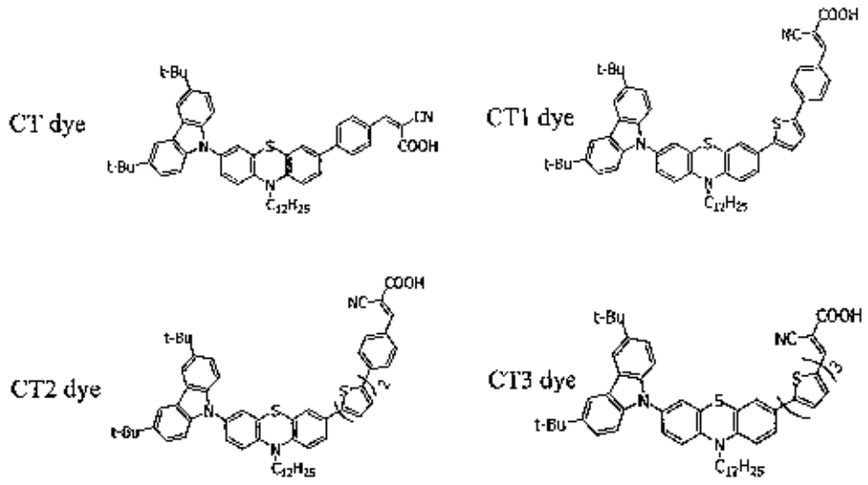

Figure 1.6 t-Butyl carbazole-phenothiazine derivatives based dye (CT-series).

1.2 Objectives

The objectives of this work were divided into two parts. The first part was the methodical fabrication of the TiO_2 electrode exploring the optimal cell design, while analyzing the influence of various technical procedures on the photovoltaic performance of highly efficient DSSCs. The second part of this project was developed new dye derivatives from some simple well-known organic dyes and experimentally determine the efficiency of DSSCs based on titanium dioxide. The novel organic dye was used as the sensitizer for the large size DSSCs modules.

CHATER 2

LITERATURE REVIEWS

This Chapter will provide all of the background information and literature review on the solar energy background, the dye sensitized solar cells, the photovoltaic cell performance, the incidence photon to current conversion efficiency, the basic component and the strategy for DSSCs development. In additional, the focus on the modification and apply of organic dye in DSSCs are explained.

2.1 The Dye sensitized solar cells

2.1.1 Background

Dye sensitized solar cells (DSSCs) have aroused much attention as a cheap and next generation solar cell. It is well known that a typically DSSCs consists of porous TiO_2 film, dye molecules which are sensitive to sunlight, and an organic liquid electrolyte, essentially containing iodide and triiodide ions as a redox couple [30, 31]. These three layers are sandwiched together between two conducting glasses, one covered with a thin layer of TiO_2 and the other with a platinum layer. DSSCs show considerable potential as a relatively low cost alternative to silicon based solar cells. These cells were developed by Grätzel and coworkers in 1991 with an impressive overall efficiency higher than 7%, using a ruthenium based sensitizer and a porous TiO_2 layer as the semiconductor material [32]. In the case of conventional DSSCs, the DSSCs as an alternative to conventional Si-based solar cells because of their several advantages such as transparency, efficiency comparable to that of an amorphous Si solar cell, color and low cost. The DSSCs has a very simple structure, photoactive anode with nano-crystalline TiO_2, Pt-coated cathode, and electrolyte in between. As a lab scale cell, its maximum efficiency has reached near 12% [33], and 10% in sub-modules [34]. Another attractive feature has been the enhanced performance under real outdoor conditions or indoor applications (relatively better than competitors at diffuse light and higher temperatures). Other advantages for DSSCs also include flexibilities in the designs (transparency and multicolor options for building integration and

consumer products), lightweight, short energy payback time (<1 year), bifacial cells capturing light from all angles, etc. Although the efficiencies of DSSCs at the present stage are lower than those conventional solar cells, the high ratio of the performance/price still identifies DSSCs as an attractive potential solar cell technology to be commercialized [35].

2.1.2 Solar irradiation and availability of solar electricity

The intensity of solar radiation in the earth's distance from the sun is approximately 1353 kWh m^{-2}, a number also called ***the solar constant***. The solar radiation is emitted from the sun's photosphere at 6000 K temperature, which gives it a spectra distribution resembling closely that of a black body at the corresponding temperature. Passing through the earth's atmosphere the solar radiation is attenuated by scattering from the air molecules, aerosols and dust particles, as well as by absorption by the air molecules, in particular oxygen, ozone, water vapor, and carbon dioxide. This gives a characteristic fingerprint to the solar radiation spectrum on the earth's surface (Figure 2.1).

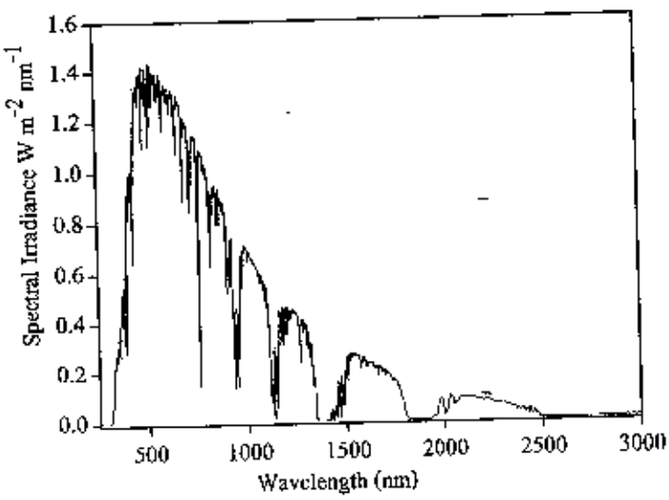

Figure 2.1 The standard AM1.5 global solar spectrum.

The available solar irradiation in a certain place depends on the latitude, the altitude and the climatic type in a yearly basis, and on the season, the time of day and the weather conditions in a specific time. The total yearly solar irradiation on horizontal surface is

700-1000 kWh m^{-2} in North Europe, 900-1300 kWh m^{-2} in Middle Europe, 1300-1800 kWh m^{-2} in South Europe, 1800-2300 kWh m^{-2} in the equator, and 2000-2500 kWh m^{-2} in the so called "solar belt" i.e. between 20° and 30° latitude.

An order of magnitude estimate of the usefulness of these yearly solar energy densities, converted to electricity with a grid-connected PV system, can be made by comparing these to an area related yearly electricity consumption of a typical detached house. In Finland, a typical of electricity consumption for a 4 person family living in a detached house with floor area of 120 m^2 and using electric heating is 18500 kWh/year. The yearly solar irradiation falling to the same horizontal area in North Europe conditions (about 1000 kWh m^{-2}/year), converted to solar electricity with total PV system efficiency of 10% amounts to about 12000 kWh m^{-2}.

2.1.3 Solar spectrum

Each second, the sun releases an enormous amount of radiant energy into the solar system. The temperature at the centre of the sun is high enough to facilitate nuclear reactions, which are assumed to be the source of the sun's energy. It emits light with a range of wavelengths from the ultraviolet (200 - 400 nm) and visible (violet, 390 nm -red, 740 nm) to the infrared (700 nm to 1 mm) [36]. (Yellow area in Figure 2.2) It peaks in the visible, resembling the spectrum of a blackbody at a temperature of 5760 K. It is, however, influenced by atmospheric absorption and the position of the sun.

As the Sun's rays pass through the atmosphere certain wavelengths are absorbed and a proportion of the total energy is scattered. Thus the solar spectrum at the Earth's surface has some wavelengths missing (Orange area, Figure 2.2) [36] and the overall intensity is reduced. In particular, ultraviolet light is filtered out by ozone, and water and CO_2 absorb mainly in the infrared making dips in the solar spectrum at 900, 1100, 1400, and 1900 nm (H_2O) and at 1800 and 2600 nm (CO_2), respectively.

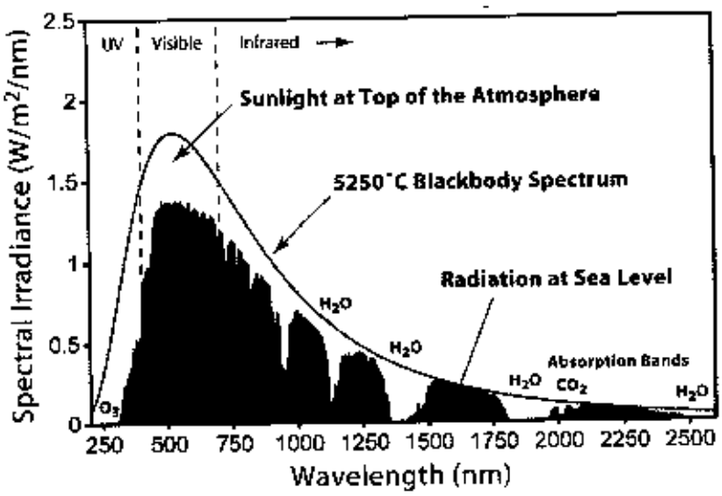

Figure 2.2 The solar spectrum at the Earth's surface.

The amount of energy reflected, scattered and absorbed depends on the amount of atmosphere that the incident radiation travels through as well as the levels of dust particles and water vapor present in the atmosphere. The latter is difficult to judge but the distance travelled through the atmosphere by incident radiation depends on the angle of the Sun. This distance is the shortest when the sun is at the zenith, i.e. directly overhead. The ratio of an actual path length of the sunlight to this minimal distance is known as the optical air mass. When the sun is at its zenith the optical air mass is unity and the radiation is described as air mass one (AM1) radiation. When the sun is at an angle θ to the zenith, the air mass is given by the equation:

$$\text{Air mass} = (\cos\theta)^{-1} \tag{2.1}$$

AM0 radiation is the extraterrestrial spectrum of solar radiation outside the Earth's atmosphere, which power density is the solar constant. Opposed to the situation outside the Earth's atmosphere, terrestrial solar radiation varies both in intensity and spectral distribution depending on the position on the Earth and the position of the sun in the sky. In order to allow comparison between the performances of solar cells tested at different locations, a terrestrial solar radiation standard has to be defined and measurements referred to this standard. The standard solar spectrum used for efficiency measurements of solar cells is AM 1.5 G (global), corresponds to an angle of 48.2 degrees between the Sun's position and the zenith (Figure 2.3).

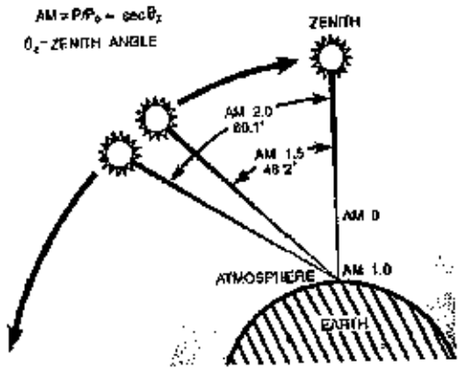

Figure 2.3 The Sun's position and the zenith.

This spectrum is normalized so that the integrated irradiance (the amount of radiant energy received from the sun per unit area per unit time) is 1000 W m^{-2}. The standard solar spectrum used for efficient AM1.5 G (global) radiation serves at present as the standard spectral distribution. The irradiance varies depending on the position of the Sun, orientation of the Earth, and sky conditions. We can also distinguish sunlight in direct or diffuse light. The direct component can be concentrated, which increases the solar cell efficiency by increasing cell voltage outputs. Diffuse light arises by scattering of the sunlight in the atmosphere. This fraction is around 15% on average but larger at higher latitudes and in regions with a significant amount of cloud cover. Materials with rough surfaces such as DSSCs are relatively better suited for diffuse light than perfectly flat surfaces and are less sensitive to movements of the sun.

2.2 Photovoltaic cell performance

A photovoltaic cell is a device, which converts incident light to electrical energy. Generation of electrical power under illumination is achieved by the capability of the photovoltaic device to produce voltage over an external load and current through the load at the same time. This is characterized by the current-voltage (*IV*) curve of the cell at certain illumination and temperature (Figure 2.4).

When the cell is short circuited under illumination, the maximum current, the short circuit current (I_{sc}), is generated, while under open circuit conditions no current can flow and

the voltage is at its maximum, called the open circuit voltage (V_{OC}). The point in the *IV*-curve yielding maximum product of current and voltage, i.e. power, is called the maximum power point (*MPP*). Another important characteristic of the solar cell performance is the fill factor (*FF*), defined as

$$FF = \frac{V_{MPP} I_{MPP}}{V_{OC} I_{SC}} \tag{2.2}$$

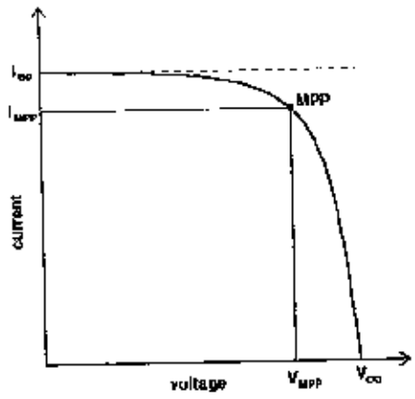

Figure 2.4 Typical shape of the current-voltage curve of a photovoltaic cell showing the open-circuit voltage V_{OC}, short-circuit current I_{SC}, and the maximum power point MPP, and the current and voltage at the *MPP*: I_{MPP}, V_{MPP}.

FF is an indication of how close J_{mpp} and V_{mpp} come to the boundaries of power production of J_{SC} and V_{OC} and also indication of the sharpness of the bend in the exponential *J-V* curve that connects J_{SC} and V_{OC}. Since higher *FF* is related to higher maximum power, high *FF* is desired; however, the diode-like behavior of solar cells results in *FF* always being less than one. Devices with high $|J_{SC}|$ and V_{OC} can still have low *FF*, suggesting that something must be done to improve device quality.

The most discussed performance parameter of a solar cell is the power conversion efficiency η and is defined as the percentage of incident irradiance I_t (light power per unit area) that is converted into output power. Because the point where the cell operates on the *J-V* curve changes depending on the load, the output power depends on the load. For consistency, the maximum output power is used for calculating efficiency. In equation form, efficiency is written.

$$\eta = \frac{J_{max} \times V_{max}}{i_L} \times 100\% = \frac{FF \times J_{sc} \times V_{oc}}{I_L} \times 100\% \qquad (2.3)$$

This form clearly shows that FF, J_{sc} and V_{oc} all have direct effects on η. Furthermore, the area used to calculate J can affect η and should include inactive areas that are integral to the solar cell, such as grids and interconnects, when calculating efficiency for large area devices or modules.

Power conversion efficiency is important since it determines how effectively the space occupied by a solar cell is being used and how much area must be covered with solar cells to produce a given amount of power. Since larger areas require more resources to cover with solar cells, higher η is often desirable. However, there are tradeoffs between η and cost for each solar cell technology that must be balanced.

Power conversion efficiency is also very dependent on the power and spectrum of the light sources since solar cells do not absorb and convert photons to electrons at all wavelengths with the same efficiency. To draw comparisons between various solar cells, a standard spectrum must be chosen for the calculation of η. Although the spectrum of the sunlight at the earth's surface varies with location, cloud coverage, and other factors, the AM1.5 G spectrum in Figure 2.5 is the most commonly used standard spectrum for measuring and comparing the performance of photovoltaic that are intended for outdoor use. Because of difficulties recreating this exact spectrum in the laboratory with standard lamps, power conversion efficiency measurements must often be corrected based on the external quantum efficiency.

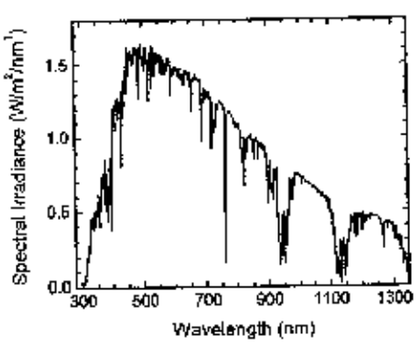

Figure 2.5 Spectral irradiance of the AM1.5 G solar spectrum up to 1,350 nm.

2.3 Incident photon to current conversion efficiency (IPCE)

IPCE is one of the fundamental measurements of the performance of the solar. It is also known as the "external quantum efficiency" and describes how efficiently the light of a specific wavelength is converted to current i.e. (electrons out) / (photons in). The IPCE can be calculated according to equation (2.4):

$$IPCE(\%) = \frac{1240 \cdot J_{sc}}{\lambda \phi_{in}} \cdot 100 \qquad (2.4)$$

J_{sc} is the short circuit current density, λ is the wavelength of the incident light and ϕ_{in} is the intensity of the incident light. The factors determining the IPCE can be expressed as:

$$IPCE = \text{LHE}.\phi_{inj}.\eta_{reg}.\eta_{cc} \qquad (2.5)$$

LHE is the light harvesting efficiency, ϕ_{inj}, η_{reg}, and η_{cc} are the quantum yield of charge injection, dye regeneration and charge collection efficiency, respectively.

The cell performance, that is, solar-to-electric conversion efficiency, is determined by the short-circuit photocurrent (J_{sc}), open-circuit photovoltage (V_{oc}), and fill factor (FF) under a definite intensity of light such as the AM1.5 solar spectrum. J_{sc} can be increased by raising the light-harvesting efficiency (LHE), that is, light absorbance by the dye-sensitized TiO_2 film. For the cell employing sensitizer dye, *cis*-(2,2'-bipyridyl-4,4'dicarboxylate)$_2$(NCS)$_2$ruthenium(II), an incident photon-to current conversion efficiency (IPCE) was near unity in the 400-550 nm wavelength range, which in turn indicates that the LHE is also near unity in the same wavelength range (156). It has been know that the power conversion efficiency (η) of a DSSC is strongly related to the light harvesting efficiency (LHE) of the dye sensitizers. The LHE has been estimated using Eq. (2.6):

$$\text{LHE}(\lambda) = 1\text{-}10^{-\text{Abs}(\lambda)} = 1\text{-}10^{-\varepsilon(\lambda)\Gamma} \qquad (2.6)$$

where, *Abs* is the absorbance of the dye adsorbed on TiO_2 film at wavelength λ, ε is molar extinction coefficient at wavelength λ and Γ is the adsorption capacity onto the TiO_2 photoanode (the dye uptake).

2.4 Materials development of DSSCs

The operation of DSSCs can be improved by development working electrode (TiO_2-electrode) with high dye loading, design dye-molecule with high light-harvesting, counter electrode with high stability and electrolyte with matching with dye. So, the material development is reviewed.

2.4.1 Mesoporous, nanostructured oxide (semiconductor) electrode

The nanocrystalline materials have recently attracted much attention owing to their peculiar physical and chemical properties [37]. Among wide-band gap metal oxides such as zinc oxide, tin oxide and titanium dioxide [38, 39], nanocrystalline titania is most promising material for electrode of dye-sensitized solar cell (DSSCs) as the position of the conduction band edge of the titania suitable allows electron injection from the excited state of the dye. TiO_2 leads to the highest DSSCs efficiency.

TiO_2 is a stable, non-toxic oxide, occurring naturally through a variety of crystal structures including anatase, rutile, and brookite. Rutile is the most stable from a thermodynamic point of view. Anatase however is the preferred structure in DSSCs, because of a larger bandgap (3.2 eV vs 3.0 eV for rutile), and a higher conduction band edge. This leads to a higher Fermi level and V_{OC} (open-circuit voltage, which is the difference between the semiconductor Fermi level and the redox potential of the electrolyte).

Thus, to preparation titanium dioxide thin film, a number of methods have been reported such as chemical vapor deposition, hydrothermal, DC magnetron sputtering [40] and sol-gel method [41]. The sol-gel methods have been widely applied for the preparation of thin films in comparison with vapor-phase methods because of their relatively inexpensive manufacturing cost.

The mesoporous TiO_2 electrode was prepared by micro-plasma oxide method (MPO) for DSSCs, that shown suitable preparation of working electrode at 20 A dm^{-2}. The open-circuit voltage and the short-circuit currents are 605 mV and 165 μA cm^{-2}, respectively. Also, using MPO to produce TiO_2 electrode is propitiated to fabrication of the large area dye-sensitized solar cells [42]. The application of nanoporous titanium dioxide to DSSCs was enhanced considerably compared with that using nanometer sized TiO_2 prepared using a hydrothermal method. The energy conversion efficiency of the DSSCs prepared from nanoporous structured TiO_2 was approximately 8.71% with N719 dye under 100 mW cm^{-2} simulated light.

That explained by the electron density and flow of electrons on the DSSCs film from roughness analysis in the AFM images [43]. The novel TiO_2 nanorod/nanoparticle (NR/NP) bilayer electrode was synthesized by sol-gel method, in Honda Hafez research group [44]. The new NR/NP bilayer design that can posses the advantages of both building blocks, ie, the high surface area of NP aggregates and rapid electron transport rate and the light scattering effort of single-crystalline NRs. The influence of TiO_2 nanocrystals were applied in Puheng's work [45]. The morphology and size of TiO_2 nanorystals can effect on the UV-vis and FT-IR spectra of the sensitized anchored on their surface. The main reason is that the morphology and the size of TiO_2 nanocrystals can affect the energy level binding mode between the N719 and the TiO_2. Shantikumar Nair and co-worker tried to improvement the DSSCs efficiency by using TiO_2 nanotube [30]. The using of TiO_2 nanotube length shows a good lateral spacing could significantly improve the performance of back illuminated DSSCs. By employing the TiO_2 nanotube array anodized at 24 h showing a diameter ~ 80 nm and length ~ 15 μm as the photo-anode for back illuminated DSSCs, a full-sun conversion efficiency (η) of 3.5% was achieved.

The enhancement of dye-sensitized solar cells by using graphene-TiO_2 composites as photoelectrochemical working electrode was studied by Tsung-Hsuan and colleague [46]. The composite films of graphene-content TiO_2 were deposited on indium tin oxide (ITO) substrates by spin coating at room temperature and applied as working electrodes of dye-sensitized solar cells (DSSCs). The amount of dye absorption is increased with increase in the content of graphene and cyclic voltammetry (CV) measurement show a gradual increase in the anodic content. The optimum content of grapheme (1 wt%) involve in TiO_2 film, a 15% improvement in the cell efficiency (from 5.98% to 6.86%) is achieved. The Korea researcher tried to improvement the DSSCs efficiency by using of mesoporous S-N-codoped TiO_2 loaded with Ag nanoparticles [47]. Mesoporous S-N-codoped TiO_2 photocatalyst loaded with Ag nanoparticles (NPs) were synthesized via a facial photochemical deposition approach. The samples possessed a homogeneous pore diameter and a high surface area 53.3 $m^2 g^{-1}$ for the Ag-loaded S-N-codoped TiO_2-*vis* samples, which facilitated the great enhancement of adsorption capacity for dye methyl orange (MO) molecules. The present photocatalytic system with noble metal-loaded TiO_2 and mesoporous structure might be good candidates to convert abundant visible of solar light energy into useful chemical energy. Because of the efficient visible light absorption capability and prominent adsorption capacity, the noble metal modification of nonmetal-doped TiO_2

nanocomposites might be used for other photo-applications such as photoelectrochemical cells, solar cells, and photocatalysts for hydrogen production.

The study compares the visible light reactivities and properties of two sensitized Pt/TiO_2 photocatalyst ($Pt/TiO_2/RuL_3$) on which ruthenium bipyridyl complexes (RuL_3) are anchored through carboxylic (c-RuL_3) or phosphonic (p-RuL_3) acid groups [48, 49]. The surface complexes of c-RuL_3 and p-RuL_3 were shown in Figure 2.6. The Pt/TiO_2/p-RuL_3 exhibited consistently higher visible light reactivities in waters than Pt/TiO_2/c-RuL_3 for all tested reactions and conditions, despite the fact that p-RuL_3 has a lower visible light absorptivity than c-RuL_3.

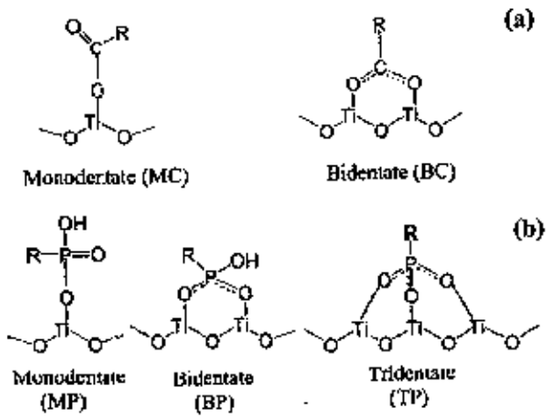

Figure 2.6 Structures of the possible surface complexes of (a) c-RuL_3 and (b) p-RuL_3 anchored on TiO_2 [48].

Tsoukleris and co-worker [50] suggested the screen-printed titania films for dye-sensitized solar cells. The screen printing of titania pastes based on 2-ethylhexanol and commercially available TiO_2 powder (Degussa P25) leads to development of nanostructured, and high surface area TiO_2 thin films, with increased surface roughness and complexity, homogeneity, compact structure without crack/defects and good adherence on the conductive glass substrate. The screen printing schematic was shown in Figure 2.7 [50].

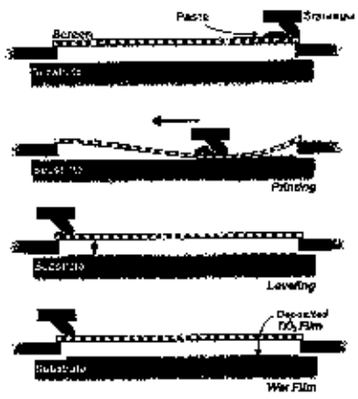

Figure 2.7 Schematic representation of the screen-printing process [50].

For further improvement of cell's performance, a combination of changes including fine tuning of the film thickness and surface properties (*via* better optimization of the screen printer conditions, mainly screen mesh, air pressure, printing speed, and screen-substrate distance) as well as higher firing temperature are necessary.

2.4.2 Dye

The molecular structure of the dye plays an important role in DSSCs. After absorption of light, charge separation is generally initiated at the interface between the dye bound to the TiO_2 surface and the hole-transporting material. The performance of DSSCs generally depends on the relative energy levels of the sensitizers and the kinetics of the electron-transfer processes at the interface between the dye bound to the semiconductor surface and the hole-transporting material. Some general principles to construct an efficient dye and efficient DSSCs are as follows [51]:

2.4.2.1) The absorption spectrum of the photosensitizer should cover the whole visible region and even the part of the near-infrared (NIR).

2.4.2.2) The photosensitizer should have anchoring groups (-COOH, $-H_2PO_3$, $-H_2SO_3$, etc.) to strongly bind the dye onto the semiconductor surface.

2.4.2.3) The excited state level of the photosensitizer should be higher in energy than the conduction band edge of the semiconductor, so that an efficient electron transfer process between the excited dye and conduction band of the semiconductor can take place.

2.4.2.4) For dye regeneration, the oxidized state level of the photosensitizer

must be more positive than the redox potential of electrolyte.

2.4.2.5) The photosensitizer should be photostable, and electrochemical and thermal stability are also required.

The sensitizers used in DSSCs are divided into two types, *viz.*, organic dyes and inorganic dyes according to the structure. Inorganic dyes include metal complexes, such as polypyridyl complexes of ruthenium and osmium, metal porphyrin, phthalocyanine and inorganic quantum dots, while organic dyes in clued natural and synthetic organic dyes.

Compared with organic dyes, inorganic metal complex dyes have high thermal and chemical stability. Among these complexes, polypyridyl ruthenium sensitizers were widely used and investigated for their high stability and outstanding redox properties and good response to natural visible sunlight [51].

Metal complexes and ruthenium (Ru(II)) complexes, in particular, have been investigated intensively for DSSC application because of their broad absorption spectra and favorable photovoltaic properties. Generally, metal complex photosensitizers consist of a central metal ion with ancillary ligands having at least one anchoring group. Light absorption in the visible part of the solar spectrum is due to a metal to ligand charge transfer process. Anchoring groups are employed to link the dye with the semiconductor and facilitate the injection of the excited electron into the conduction band of the semiconductor. One can modify any part of the complex to tune the energy levels of the metal to ligand charge transfer process and to optimize electron injection and regeneration kinetics [52].

Most well known Ru-complexes for DSSCs are N3, N719, N749 and Z907 [52]. The dye structures were shown in Figure 2.8.

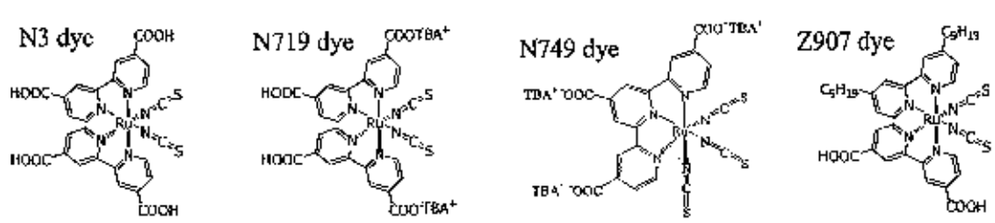

Figure 2.8 The molecular structures of ruthenium (Ru(II)) complexes dyes [52].

The N3 (*cis*-di(thiocyanato)-bis(2,2'-bipyridyl-4-4'-dicarboxylic acid) ruthenium(II)), that has several advantages when used as a sensitizing dye, including a broad range of visible light absorption and demonstrated stability over many hours of cell operation [53]. N3 has two bipyridine and two isothiocyanato (NCS^-). It absorbs up to 800 nm radiation due to the loosely attached NCS group. Even though, the dye provides the high J_{SC} (short circuit current), that give low V_{OC} [54]. The N3 is a paradigm in this field; the efficiency using relatively thick TiO_2 films under standard air mass 1.5 reporting conditions stands presently at 10% [55]. However, the hydrophilic terminal and light-capturing ability of this sensitizer proved unsatisfactory in permitting DSSCs devices to achieve robust stability and higher photovoltaic performance. This initial time period these drawbacks have been successfully addressed with significant improvement of these criteria through the embodiment of two well–known ruthenium complexes are N719 and Z907 [56].

N719 has the same structure as N3 dye but has TBA^+ (tetrabutylammonium) instead of H^- at two carboxyl groups. The difference in V_{OC} is rationalzed as due to the difference in proton concentrations at the surfaces which has been so far the most successful dye for DSSCs. [51]. Z907 has different features than others. DSSCs using N3 and N719 have shown degradation during long-term operation. This is because water molecules penetrate into the electrolyte and desorbed the dyes from the TiO_2 surface [57]. Z907 has hydrophobic alkyl chains attached to one of the bipyridine ligands and it keeps water molecules away from the chemical bonds between the dye and TiO_2. The conversion efficiency of Z907 was reported by Wangdong Zeng et al. of 7.2% base on solvent-free ionic liquid electrolyte EL02 (DMII/EMII/EMITCB/I_2/GNCS; molar ratio:12/12/16/1.67/3.33/0.67) [58, 59].

In recent years, interest in metal-free organic dyes as an alternative to noble metal complexes has increased due to their many advantages, such as diversity of molecular structures, high molar extinction coefficient, and simple synthesis as well as low cost and environmental benefits [58]. Organic dyes with large π-aromatic such as coumarin [59], phenothiazine [60], benzothiadiazole [61], triphenylamine [62], perylene, thiophene [63] and porphyrin [64] derivatives, have been investigated as sensitizers in DSSCs.

Porphyrins are one of the most widely studied sensitizers for DSSCs because of their strong Soret (400-450 nm) and moderate Q bands (550-600 nm). The porphyrin-based dyes have several intrinsic advantages, such as the good photostability prefered by the natural

chlorophylls, their rigid molecular structures with large absorption coefficients in the visible region, and their many reaction sites, that is, four meso and eight beta positions, available for functionalization. Kang Deu Seo and et al. further designed and synthesized the novel zinc porphyrin dyes which have D-π-A system base on porphyrin derivatives containing a triphenylamine (TPA) electron-donating group and a phenyl carboxyl anchoring group substituted at the meso position of the porphyrin ring [58]. The HKK-Por dye structures were shown in Figure 2.9.

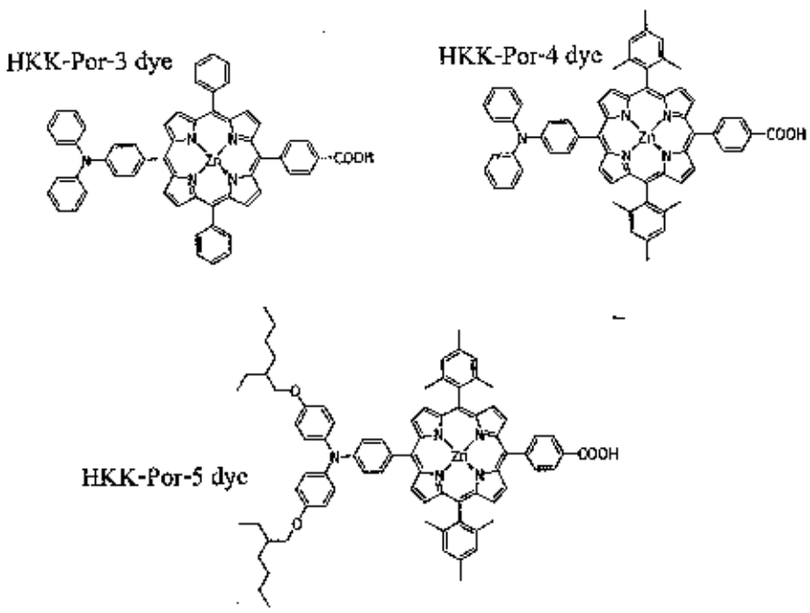

Figure 2.9 The molecular structures of HKK-Por dyes [59].

A maximum photon-to-electron conversion efficiency of 3.36% was achieved with the DSSCs based on HKK-Por5 dye due to the introduction of the alkoxy group in to the TPA moiety at the meso position of porphyrin ring (J_{sc} = 9.04 mA cm^{-2}, V_{OC} = 0.57 V, FF = 0.66; under AM1.5 irradiation (100 mW cm^{-2})).

The novel meso- or β-derivatized porphyrins with a carboxyl group were designed and synthesized by Cheng-Wei Lee and et al. [65], the molecular structure of porphyrin 5 was shown in Figure 2.10. From a comparison of the cell performance based on the same TiO_2 films, the devices made of porphyrin 5 co-adsorbed with chenodeoxycholic acid (CDCA) on TiO_2

in ratios Dye/CDCA = 1:1 and 1:2 have efficiencies of power conversion similar to that of an N3-based DSSCs.

Porphyrin 5 dye

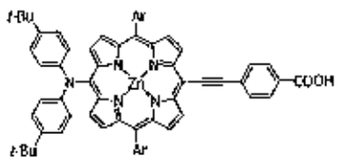

$\eta\% = 6.00$

V_{OC} =0.71 V

J_{SC} = 14.33 mA cm^{-2}

$FF = 0.59$

Figure 2.10 The molecular structure of Porphyrin 5 [65].

Hseu-Pei Lu had reported the photovoltaic performance and kinetics of femtosecond fluorescence of three zinc-porphyrin sensitizer (YD0-YD2) [65]. The dye structures were shown in Figure 2.11.

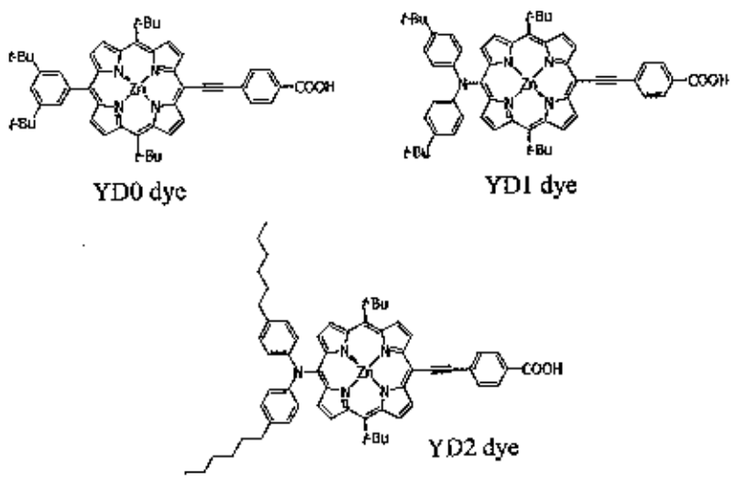

YD0 dye

YD1 dye

YD2 dye

Figure 2.11 The molecular structures of zinc porphyrin sensitizer YD0-YD2 [65].

The cell performances were optimized on TiO_2 films of ~ 10-μm thickness with a scattering layer of ~ 4-μm thickness: the efficiencies of power conversion of YD1 and YD2 are slightly smaller than, but near, that of N719, being 6.5% and 6.8%, respectively, compared to 7.3%. Without a scattering layer on the films, the performance of N719 was degraded significantly (6.3%), whereas the efficiencies of YD1 and YD2 decreased only slightly (6.4% and 6.5%), making this series of green sensitizers promising candidates for future light-penetrable photovoltaic applications [65].

The new donor-π-acceptor (D-π-A) metal-free-organic dyes, in which denditric triphenylamine acts as donor, and furan, thiophene and benzene as π-linkers, were synthesized, characterized and used for the application of dye sensitized solar cells (DSSCs) by Junhui Jia and et al [66]. Among the fabricated DSSCs, the device based on the furan as π-linker exhibited a short circuit current density of 14.56 mA cm^{-2}, and open circuit voltage of 0.71 V and a fill factor of 0.59, implying a power conversion efficiency (η) of 6.10%. The devices sensitized by dyes with thiophene and benzene as π-linker possessed relative lower η 5.92% and 4.97%, respectively. The results suggests that the introduction of furan and thiophene as a π-spacer increases the efficiency of DSSCs. The molecular structures of TT, TT1, TT2 and TT3 were shown in Figure 2.12.

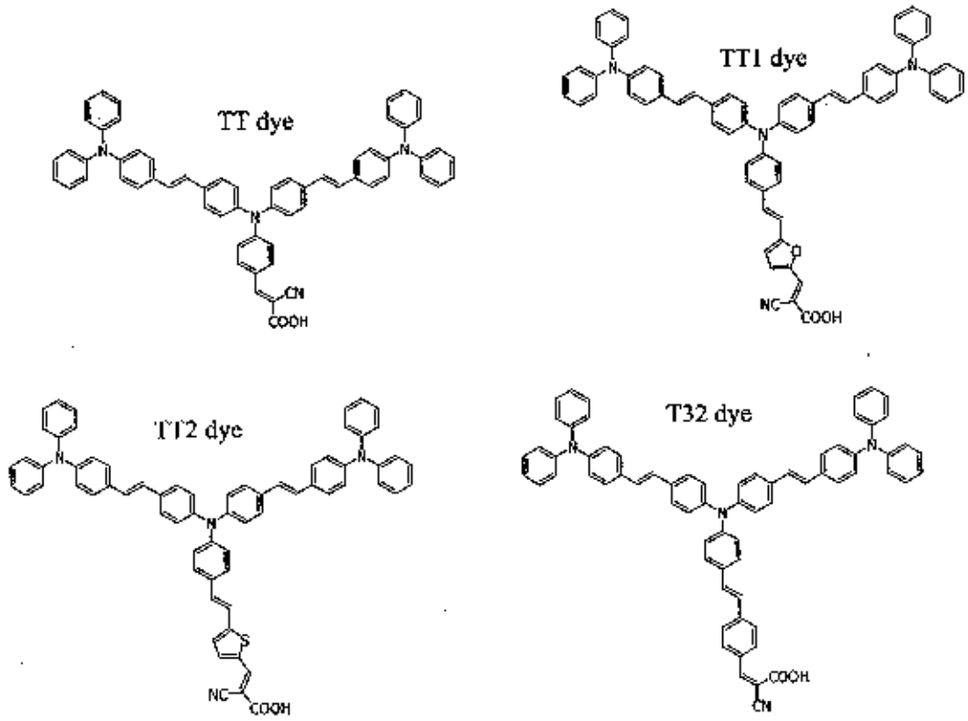

Figure 2.12 The molecular structures of TT, TT1, TT2 and TT3 [66].

The thiophene unit was applied in the various works. The comparison spacer unit between thiophene and triphenylamine moiety were studied by Ki-Hyum Kim and et al [67]. The dye structures were presented in Figure 2.13. The thiophene unit and triphenylamine were introduced as a π-conjugated bridge. The H-PTZ-TPA-T-sensitized cell showed the highest overall conversion efficiency of 4.01% (J_{SC}: 9.64 mA cm^{-2}, V_{OC}: 0.69 V, *FF*: 0.60), while the H-

PTZ-sensitized cell showed the lowest value of 3.57% (J_{SC}: 7.76 mA cm^{-2}, V_{OC}: 0.70 V, *FF*: 0.65) among the cells based on the three organic dyes compared to 5.09% for the cell based on the N719 dye (J_{SC}: 12.77 mA cm^{-2}, V_{OC}: 0.72 V, *FF*: 0.55) under AM1.5 illumination (100 mW cm^{-2}). According to the results, the measurement of photovoltaic properties to confirm the effects of π-conjugated bridge of the dye on the performance of the DSSCs. The V_{OC} value is influenced by blocking the I_3^- in electrolyte approaching the TiO_2 surface. Also, the J_{SC} value increases with increasing π-conjugated bridge length. The device show the possibility of the replacement of the ruthenium complex dyes using phenotiazine based sensitizers in the dye sensitized solar cells especially due to a cheap price of phenilthiazine.

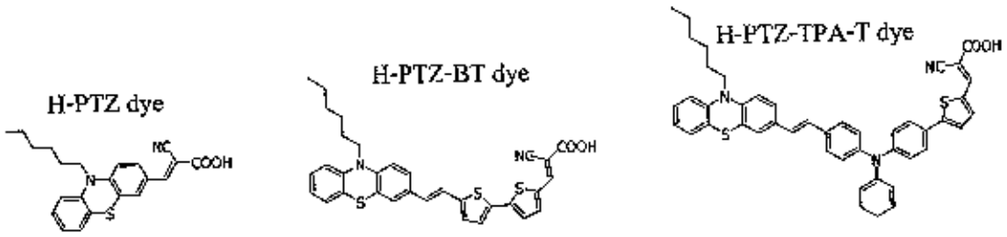

Figure 2.13 The structures of the organic dyes H-PTZ, H-PTZ-BT and H-PTZ-TPA-T [67].

The research of Wenjun Wu and et al. introduced phenotiazine in the three organic dye derivatives [60]. For three dyes, the phenothiazine derivative moiety and the cyanoacetic acid take the role of electron donor and electron acceptor, respectively. The molecular structures of P1, P2 and P3 were shown in Figure 2.14. The P2 molecule showed the best photovoltaic performance of 4.41% (J_{SC}: 10.84 mA cm^{-2}, V_{OC}: 0.59 V and *FF*: 0.69) due to its broader photo current action spectra (Figure 2.15).

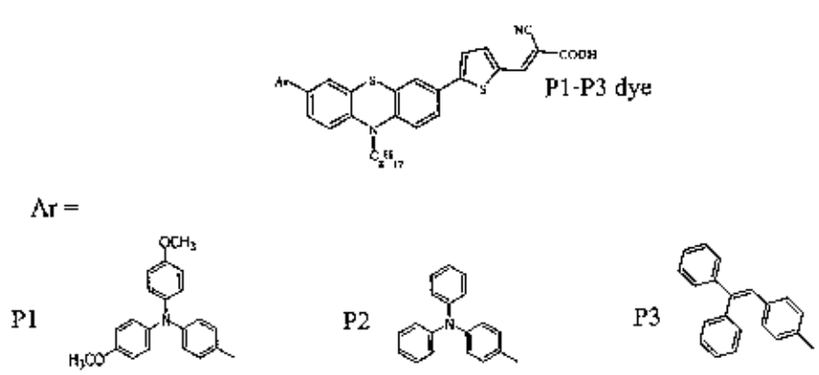

Figure 2.14 The molecular structure of dyes (P1, P2 and P3) [61].

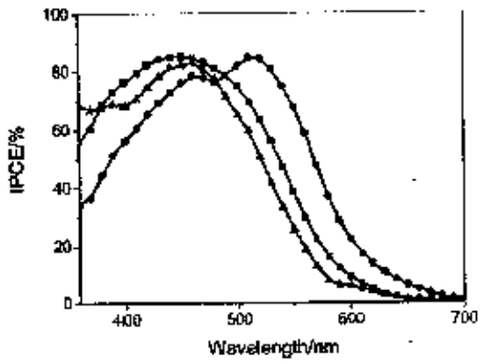

Figure 2.15 Photocurrent action spectra of the TiO_2 electrodes sensitized by P1 (■), P2 (●) and P3 (▲) [60].

Figure 2.15, all the three dyes can efficiently convert visible light to photocurrent in the region from 350-700 nm. The IPCE spectrum of P1-P3 is red shifted. This important red shift in the photocurrent respond is attributed to lateral interaction in the adsorbed layer of the sensitizer. In 2011 [68], Wenjun Wu and et al. studied the effect of chenodcoxyxholic acid (CDCA) additive on the two organic dyes containing phenothiazine and triphenylamine segments (P1 and P2). It was found that the coadsorption of CDCA can hinder the formation of dye aggregation and improve electron injection yield and thus J_{SC}, which is attributed to the decrease of charge recombination. The PCE action spectra of the TiO_2 film exposed to the dye alone and to both the dye and CDCA with 5, 10 and 20 mM in the dye solution was compared in Figure 2.16.

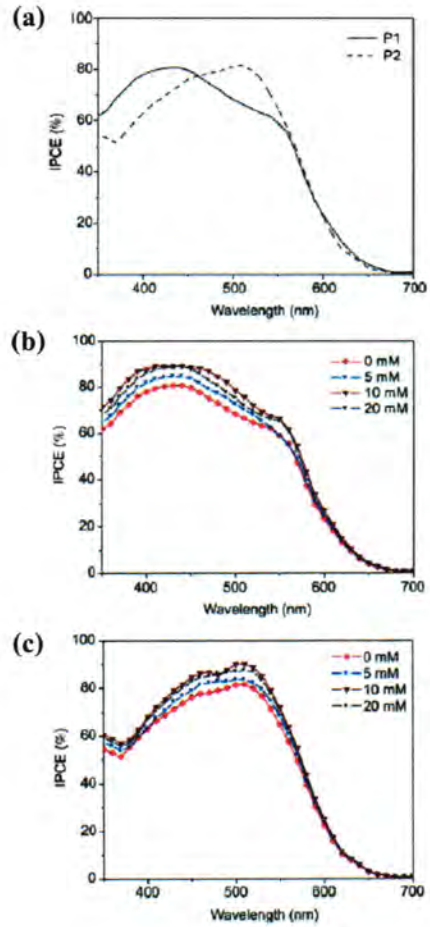

Figure 2.16 (a) IPCE spectra for P1 and P2 based DSSCs without CDCA and (b, c) dependence of IPCE on the concentration containing 0, 5, 10 20 mM CDCA [68].

From the Figure 2.16, the CDCA is known to improve DSSCs efficiency due to its preventing dye aggregation, resulting in improved electron injection efficiency, and thus leading to increase in the device photocurrent.

The double donor-acceptor (D-A) branched dye (DBD) phenothiazine unit as electron donor and a 2-cyanoacrylic acid unit as electron acceptor were synthesized and used as sensitizers for DSSCs in the work of Derong Cao and et al. [70]. That presented the conversion efficiency of the DSSCs amounts up to 4.22% (2.91% for single D-A branched). The dye structures were shown in Figure 2.17.

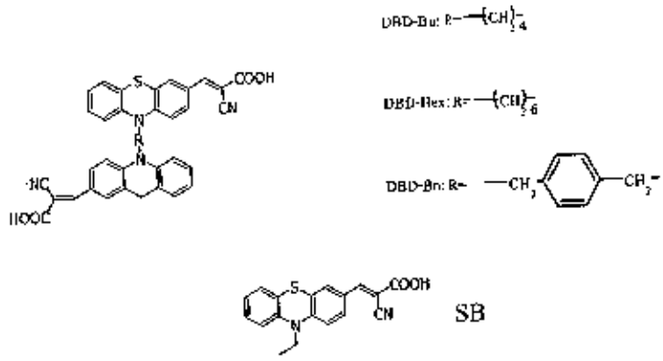

Figure 2.17 The dye structures (DBD-Bu, DBD-Hex, BDB-Bn and SB) [69].

Phenothiazine was selected as an electron donor D on the basis of the following reasons: (1) the heterocyclic compound contains electron-releasing nitrogen and sulfur heteroatoms; (2) the phenothiazine ring is nonplanar and therefore can impede the molecular aggregation and the formation of intermolecular excimers [69].

Another strategy, the improvement DSSCs efficiency used different acceptors. The work of Zhongquan Wan and et al. studied the effect of different acceptors groups (cyanoacetic acid and rhodinine-3-acetic acid; Figure 2.18) in phenothiazine-triphenylamine [70]. The conversion efficiency of the solar cell based on the cyanoacetic acid acceptor moiety was improved. The lower efficiency of solar cells based on rhodinine-3-acetic acid due to the delocalized of the excited state is broken.

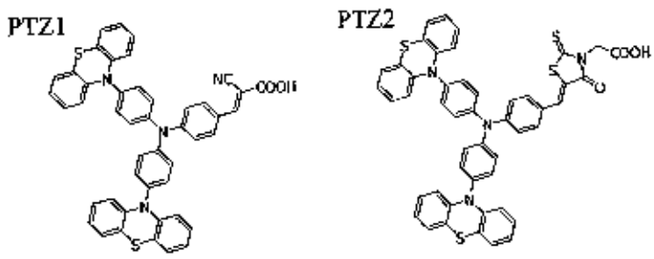

Figure 2.18 Molecular structures of PTZ-1 and PTZ-2 [70].

However, in the previous studies were shown that inclusion of alkyl [71-73] or bulky alkoxy [74] electron-donating substituent efficiently suppress recombination, improve the open-circuit voltage, suppress the aggregation of the sensitizers, increase the electron life time ,

and hence to increase the solar-to-electric power conversion efficiency. The hydrophobic long alkoxy aliphatic chains could also enhance the long-term stability of the solar cell through preventing water induced dye desorption from the TiO_2 surface. The functionalized organic dyes structures were shown in Figure 2.19.

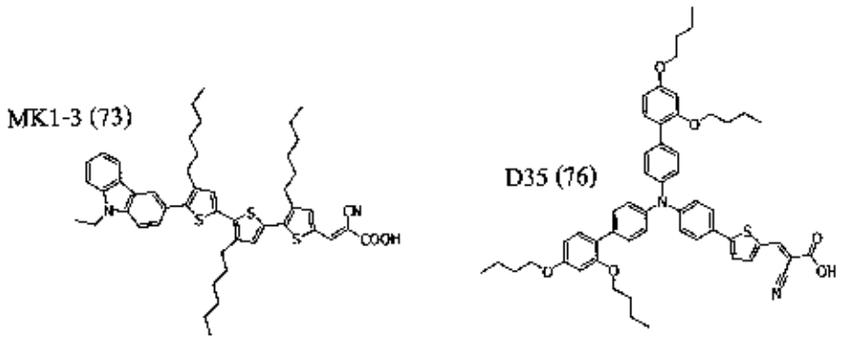

Figure 2.19 Molecular structures of MK-1 (alkyl substituent moiety) and D35 (alkoxy substituent moiety) [71, 74].

2.4.3 Electrolytes

In DSSCs, the electrolyte comprises a redox mediator. The reduced form of this mediator has to regenerate the dye ground state prior to the back electron transfer. Ideally, this redox mediator should not absorb light to prevent photon-to-current efficiency losses.

The redox couple is a key component of the DSSCs. The reduced part of the couple regenerates the photo-oxidized dye. The formed oxidized species diffuses to counter electrode, where it is reduced. The photo voltage of the device depends on the redox couple because it sets the electrochemical potential at the counter electrode. The redox couple also affects the electrochemical potential of the TiO_2 electrode through the recombination kinetics between electrons in TiO_2 and oxidized redox species [75].

The significant limitation of DSSCs to date has been the relatively low number of choices for the electrolyte [76]. So far the I^-/I_3^- couple has been most efficient and commonly used redox mediator in DSSCs, due to the fast regeneration of the oxidized dye provided by I^- on a nanosecond time scale [77]. The first DSSCs was reported in 1991 by M. Grätzel [78] using organic liquid electrolyte containing LiI/I_2, which obtained an overall light-to-electricity conversion efficiency of about 7.1% under irradiation of AM1.5, 100 mW cm^{-2}. Letter, many

kinds of liquid electrolytes containing iodide/triiodide redox couple and high dielectric constant organic solvent such as acetonitrile (AcN), ethylene carbonate (EC), 3-methoxypropiontrile (MePN), propylenecarbonate (PC), γ-butyrolactone (GBL), valeronitrile (VN) [79, 80].

Research during the decade shows the component of liquid electrolyte. One such additive is the Li ion, which is known to improve the photocurrent of DSSCs while simultaneously reducing the open-circuit voltage. It is well-known that small cations such as Li^+ are potential determining for metal oxide electrodes and that specific adsorption of Li^+ results in a positive shift of the semiconductor energy levels. The influence of lithium ion concentration on the DSSCs performance was reported [81]. The cell characteristics become progressively more "ideal" as Li^+ concentration is increase, with transfer coefficient of cal.1 for 1 M Li^+ in the electrolyte. The conduction band edge is shifted positive by increasing Li^+ ion concentrations, this positive shift in conduction band edge is also found to cause a dramatic increase in the photocurrent generation efficiency of the cells especially in the long-wavelength region of the photocurrent action spectrum.

The most convenient way to enhance the photovoltaic efficiency is the addition of appropriate chemical species in the electrolyte to fine tune the semiconductor-electrolyte interface. For instance, nitrogen heterocyclic compounds such as 4-tert-buylpyridine (TBP) was added in the electrolyte to improve the open-circuit potential (V_{OC}) but decrease short circuit current (J_{SC}), while guanidinium thiocyanate (GuNCS) was found to increase both V_{OC} and J_{SC} [80]. Therefore, Thomas Stergiopoulos and et al. reported the influence of electrolyte co-additives on the performance of dye-sensitized solar cells [83]. The co-additive composted of 4-tert-butylpyridine (TBP), N-methylbezimidazole (NMBI) and guanidinium thiocyanate (GuNCS), adsorbed onto the photoelectrode/electrolyte interface, thus shifting the semiconductor's conduction band edge and preventing recombination with triiodide. The TBP enhanced the initial efficiency under $[I_2]$ = 0.02 M from 3.5 up to 4.1%, while NMBI boosted the corresponding initial efficiency at $[I_2]$ = 0.08 M from 2.5 to 4.1%. Further addition of guanidinium cations in the above systems increased the efficiencies by another 0.5-0.7% (by increasing both V_{OC} and J_{SC}). The optimum stratification has been shown efficiencies of 5.8% with NMBI-GuNCS and up to 8.0% with TBP-GuNCS co-additives, respectively.

According to the work of Qinging Yu and et al. [80], that introduced the co-additive of TBP-GuNCS in the electrolyte as application in DSSCs based on C106-dye.

The DSSCs based C106-dye presented the conversion efficiency of 11.7-12.1% were attained at the AM1.5 conditions. On the other hand, it is only a small amount of the electrolyte electric additive into the electrolyte, the superfluous electric additive will cause a poor photovoltaic performance of DSSCs [79].

The use of liquid electrolyte is not ideal for commercial applications (especially the common use of acetonitrile derivative as the solvent), due to problems with sealing, volatility and toxicity [76]. Although iodide/triiodide has been demonstrated the most efficient redox couple for regeneration of the oxidized dye, its severe corrosion for many sealing materials, especially metals, cause a difficult assembling and sealing for a large-area DSSCs and poor long-term stability of DSSCs [77, 79]. Besides these practical problems the search for new electron transfer mediators potentially capable of replacing the I_3^-/I^- couple challenging for a number of reasons related to the strict requirements that must be fulfilled by an efficient electron mediator [77]. Therefore, other kinds of redox couples such as Br_2/Br^-, quinine/hydroquinone [84], $(SCN)_2/SCN^-$, $(SeCN)_2/SeCN$, $Co(II/III)^3$, $Cu(I/II)^4$, Fc/Fc^+, and bipyridine cobalt (II/III) complexes were investigated for use in DSSCs [85-88], owing to their energy unmatchable with dyes or their intrinsic low diffusion coefficients in electrolyte, these redox couples show lower DSSCs' light-to-electricity conversion efficiencies than the iodide/triodide redox couple does.

According the properties of liquid electrolyte, record efficiencies exceeding 11% under standard AM1.5 solar illumination have been reached with volatile electrolyte having a boiling point near 100°C. However, due to their high vapor pressure, they are difficult to use outdoor in warm climates; hermetic sealing requirements pose a challenge for practical applications [88]. In the decade, much attention has therefore been paid to the development of non-volatile electrolytes meeting the stability requirements for outdoor applications. Room-temperature ionic liquid (RTIL) has good chemical and thermal stability vapor pressure, non-flammability, and high ionic conductivity, whereas large viscosity of the ionic liquids is a serious problem for the development of such devices using these promising solvents. [89]. Photocurrents in such systems are affected by the series resistances of the electrolytes, which are usually in proportion to the viscosity. According to the publication of Grätzel and coworkers reported [90] the use of ionic liquids, consisting of 1-hexyl-3-methylimidazolium iodide (HMImI) and I_2 as an electrolyte of DSSCs and revealed the high short-circuit currents (J_{SC}), in spite of the extremely

high viscosity. When incorporated into DSSCs, RTL can be both the source of iodide and the solvent itself.

The ionic liquids (ILs) were first used in the DSSCs in Grätzel's laboratory, with the primary aim of preventing voltage drop by the Li^+ and K^+ ions because the IL cations can replace the absorption sites on the TiO_2 surface [91]. The first IL tested in DSSCs was based on the imidazolium cation, and subsequently, ILs based on this family has been widely used in the electrolytes for DSSCs. The kinds of ionic liquids were shown in Figure 2.20.

The performance of DSSCs containing different ILs reportedly depends upon different factors: *viz*, viscosity, ionic conductivity, diffusion coefficient, size of the cation ring, number, position and length of alkyl groups, melting point, *etc*. Tae Yeon and colleague [91] studied the effect of ionic liquid with different cations (imidazolium, pyrrolidinium, piperidinium and pyridinium) on the performance of DSSCs based on electrolytes containing a TBP in 3-methoxypropioitrile (MNN).

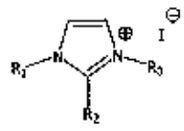

Imidazolium Iodide derivatives

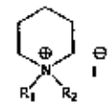

Piperidinium Iodide derivatives

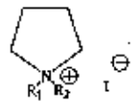

Pyrrolidinium Iodide derivatives

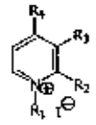

Pyridinium Iodide derivatives

Figure 2.20 The kinds of ionic liquids [91].

The ILs based on four types of 5- and 6-member ring cations have different mono-, di- and tri- alkyl groups were used in the electrolytes for DSSCs. The device containing 1-hexyl-pyridine was presented the best overall conversion efficiency of 7.21% (V_{OC} = 0.73 V, J_{SC} = 16.18 mA cm^{-2}, FF = 0.61) based on N719 dye. The length and position of the alkyl groups of the ILs were observed to have more effect on the performance of the cell than the nature of the 5- or 6- membered ring of the ILs cation.

The ILs using imidazolium cations have fared the best for the DSSCs [88, 89, 92, 93], the very high concentration of I^- (ca 5.8 M) present in the pure imidazolium iodide melts entails two other advantages, the first being a reduction of the open circuit voltage (V_{OC}) of the cell due to the lowering of the Nernst potential of the counter electrode and the second the occurrence of reductive quenching of the ruthenium sensitizer comparing with electron injection from the excited state and decreasing the short-circuit photocurrent density (J_{SC}) of the cells. These problems are alleviated by adding a low-viscosity IL having an inert anion to the iodide-containing IL. A variety of such binary ILs containing different anions have been explored, such as bis-(tripluoromethylsulfonyl) imide (Tf_2N^-), thiocyanate (NCS^-), tricyanometananide ($C(CN)_3^-$) and tetracyanoborate ($B(CN)_4^-$). The Tf_2N^- and $B(CN)_4^-$ have shown the stable performance in the DSSCs, but the 1-ethyl-3methyl-imidazolium tetracyanoborate ($EMIB(CN)_4$), whose viscosity is only 19.8 cP at 20°C was interested. The publication [88, 89] reported the effect of the binary ionic liquid electrolyte (1-propyl-3-methyl-imidazilium iodide (PMII) and 1-ethyl-3-methyl imidazolium tetracyanoborate ($EMIB(CN)_4$), that present the improvement of DSSCs performance and exhibit excellent stability [92, 93].

However, if the cells are not hermetically sealed, volatile solvents can leak out and evaporate under thermal stress, leaving only ionic liquids behind and deteriorating the device performance. Hence, it is pertinent to employ nonvolatile-free ionic liquid or polymer electrolyte. Hence, it is pertinent to employ nonvolatile solvent-free ionic liquid or polymer electrolyte or all-solid-state hole transporting materials in DSSCs. Yiming Cao and colleague [95] studied the temperature-dependent physicochemical, such as density, conductivity, and fluidity, of 1,3-dialkylimidazolium iodide. In combination with the amphiphilic Z907Na sensitizer [Figure 2.21], that found the important to use low-viscosity iodide melts with small cations to achieve high-efficiency dye-sensitized solar cells. These studies reveal that the viscosity-dependent transport of tiiodide in ionic liquid electrolytes with high iodide concentration can be explained by two parallel processes. Apart from the normal physical diffusion, the coupling process of physical diffusion and bond exchange is responsible for the observed abnormally high diffusion coefficients. The study has provided useful insight for further improvement of solvent-free electrolyte based on rational design of their constituents, facilitating the large-scale practical application of lightweight, flexible dye-sensitized solar cells.

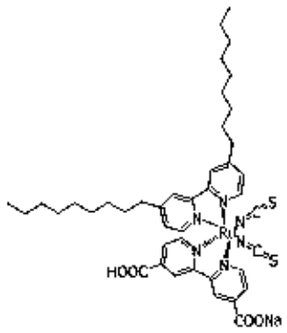

Figure 2.21 The molecular structure of Z907Na.

Beside, the solidifying electrolyte forming gel of quasi-solid-state electrolyte has been the primary solution to make the sealing process easier and to minimize the loss of electrolytes for enhanced durability. The agarose gel electrolyte was studied by Hsin-Ling Hsu and et al [95]. The environmental benign co-solvent such as dimethyl sulfoxide (DMSO)/ propylene carbonate (PC) can significantly increase the conversion efficiency to 3.4% with agarose compared to pure 1-methyl-3-propylimidazolium iodide (MPII) with agarose (1.4%), while retaining~80% of the energy conversion efficiencies of the reference cell without agorose under the illumination at AM1.5 (100 mW cm^{-2}). Zhipeng Huo and co-worker [96] reported the improvement of electrolyte for DSSCs by using quasi-solid-state Poly (vinylidenefluoride-co-hexafluorenepropylene) (P(VDF-HFP)) introduced with TiO_2 nanoperticles. These studies showed that the nano-TiO_2 composite gel electrolytes based devices could maintain 90% of their initial value after heating at 60°C for 1000 h. From the results, that was contributed significantly to improvement of the performance and long term stability of the quasi-solid-state DSSCs [97, 98].

2.4.4 Counter electrode

Generally, a DSSC is composed of a dye-sensitized mesoporous semiconductor photoanode, an electrolyte containing an iodide/triiodide redox couple, and a catalytic counter electrode (CE). One of the most important components of DSSCs is CEs which collect electrons arriving from external circuit and catalyze reduction reaction of triiodide ion. Thus, the CE should possess high catalytic activity and high electrical conductivity for efficient charge transport [99]. At the counter electrode triiodide should be efficiently reduced to iodide. The counter electrode must be catalytically active to ensure rapid reaction and low overpotential. The overpotential η needed to drive the reaction at certain current density gives rise to a charge transfer resistance (R_{CT}

$= \eta/J$), which acts as a series resistance in the solar cell: Ideally R_{CT} should be down to ~ 1 Ω cm^{-2} to avoid significant losses [75]. Many electrode materials were used as CE, such as carbon, gold, platinum and polymer. The Platinized counter electrode has been widely used in DSSC so far, due to its high conductivity and catalytic activity for reduction of I_3^- ions [100].

Therefore, most of the work on DSSCs have utilized as the cathode material. The several methods were used to preparation of CE, for example, thermal decomposition of Pt precursor [80, 81, 101], doctor blade [86], sputtering [50, 89, 95], dropping [85, 88, 90, 97, 98, 102] and spin-coating [103]. The preparation CE by dropping of Pt precursor solution on the FTO substrate is fundamental method and inexpensive. The dropping technique was applied into the work of Min-Hye Kim and colleague [102]. That reported on a method to preparation Pt electrodes with homogeneously dispersed Pt nanoparticles on FTO substrates by adding an organic additive, hydroxylpropyl cellulose (HPC) in Pt precursor solution. The distribution of Pt precursor at the surface is an important factor for the improvement DSSCs performance.

According the regeneration of dye electrons occurs through electron donation from a redox electrolyte in contact with dye. This typically occurs through an organic solvent containing an iodide/triiodide couple. Triiodide is reduced in turn at the counter electrode. Therefore, the DSSCs fabrication by using the different of counter electrode (gold and graphite) was observed [10]. Although, the FF for both cells was found to be 70%, short circuit current density and open circuit voltage for operation with graphite and gold coated counter electrodes were increased from 1.44 to 2.13 mA cm^{-2} and 360 to 370 mV, respectively. Overall conversion efficiencies (η) for fabricated cells fund to be 3.63% for cell operated with graphite and 5.51% for gold counter electrodes.

However, for cost-effective fabrication and long-term stability of the DSSC, Pt CEs suffer from its high price, rarity, and susceptibility to corrosion by iodide electrolyte. Therefore, development of Pt-free CEs using alternative materials is expected to reduce production costs of DSSCs [99], it is desirable to develop low-cost and more stable materials such as carbon, carbon black, graphite, activated carbon or single-wall carbon nanotubes and conductive polymers. Carbonaceous materials contain significant features such as high electronic conductivity, corrosion resistance toward triiodide, high reactivity for triiodide reduction and low cost [104]. Ongon Topon and et al. applied carbon nanotubes (CNT) as counter electrode for DSSCs. The counter electrode was fabricated by microwave plasma-enhanced chemical vapor

deposition (MPCVD), that the charge transport impedance of I^-/I_3^- redox reacton on a CNT counter electrode is fundamentally smaller than that of a Pt counter electrode, suggests that the CNTs directly grown on the metal substrate are promising as the counter electrode of a highly efficient DSSCs [104, 105]. Moreover, the carbon like graphene was incorporated in CE for DSSCs application due to its excellent conductivity that can decrease charge transfer resistance [107]. Josef Velten and colleague reported the replacement of the Pt catalyst normally used in DSSCs by a nanocomposite of dye spun carbon multi-walled nanotube (MWNT) sheets with graphene flakes (Gr-F) [106]. The DSSCs free of platinum that give a power conversion efficiency of 7.55%, which shows a performance 86% as efficient as the Pt reference cell.

Furthermore, the Pt-free counter electrode for low cost DSSCs was invented. Many candidates were studied the preparation of CE based on easy way and less capital. Jo-Lin Lan and et al. and Yurong Gao and colleague reported the use of carbon powder for preparation of CE paste [99, 107], with prepared by mixing with organic binder. The CE past based carbon powders showed the 93% of that of sputtered Pt CE. In addition, the applied nanocarbon powders in CE were reported by Easwaramoothi Ramasamy and co-worker. The charge transfer resistance of nanocarbon powders electrode in liquid electrolyte is 0.74 Ω cm^{-2}, which is two times less than that of screen printed platinum. The low cost DSSCs using nanocarbon CE with 6.31% energy conversion efficiency with good stability [108, 109].

Besides, the integrated materials were applied as CE for DSSCs operation, such as, poly-N-vinyl-2-pyrrolidone (PVP)-capped Pt nanoclusters (better performance for the charge-transfer resistance (R_{CT}) and the cell efficiency (η)) [110], poly(brilliant cresyl blue) (PBCB) with multi walled carbon nanotubes (MWCNT) (low cost counter electrode) [111], and Pt/carbonaceous count electrode (Pt/activated carbon and few layered graphene/Pt-nano particles; DSSC performance was superior to that for active the Pt electrode) [112, 113].

In recent years, several studies of DSSCs have employed PEDOT for preparation CE. Carbonaceous materials are quite attractive due to their high electric conductivity, corrosion resistance toward iodine, catalytic activity for the reduction of triiodide ion and low cost. However, there also is a disadvantage in that the contact between carbon particles and FTO glass is very poor [114]. Therefore, the work of Sho sakurai and et al. used ClO_4^- doped poly(3,4-ethylenedioxythiophene) (PEDOT)-supported carbon particle (PEDOT-ClO_4^-/C) composite film electrode. The electrode was prepared by electrophoretic deposition on transparent conductive

oxide glass to improve the performance of carbon-based counter electrodes for DSSCs, which is improved the FF and presented the conversion efficiency of 4.05% [115].

2.4.5 DSSCs Module

Dye-sensitized solar cells (DSSCs) have attracted considerable attention in last two decades. As the efficiency of small area DSSCs became higher and higher, many groups have made their efforts to develop large area modules [116, 122]. The confirmed highest efficiency of the large module is 9.20%, which is still apparently lower than the best small cell efficiency of 11.20% [123]. The most important cause for the lower efficiency of the modules was considered as the high resistance of the substrates [124], sheet resistance of the substrate and sealing of the electrolyte inside the cell. The most employed technique to reduce the power loss by sheet resistance is to draw conducting lines onto the substrate [125]. Silver is the most widely used material to draw conducting lines, which is often done by screen printing technique [126, 129]. According to the reported of Dong Yoon Lee in 2007 [126], the screen-printing technology is used to fabricate large dye-sensitized solar cells (DSSCs). The DSSCs module, which consists of five stripe-type working electrode on a 5 cm x 5 cm, embedded silver grid FTO glass substrate, show stable performance with an energy conversion efficiency of 5.45% under standard test conditions. The photographs of DSSCs on 5 cm x 5 cm FTO glass substrate as shown in Figure 2.22.

(a) (b)

Figure 2.22 The Photographics of DSSCs on 5 cm x 5 cm FTO glass substrate with (a) plain-type and (b) stripe type working electrode [126].

In 2008, the grid type dye-sensitized solar cell module with carbon counter electrode was reported [127]. The 5 cm x 5 cm size carbon counter electrode module with an active area of 11.2 cm^2 shows V_{OC}: 0.73 V, I_{SC}: 118 mA, *FF*: 0.55 with 4.23% active area

efficiency, which is comparable to 5.26% of platinum counter electrode module, shows that carbon can be successfully used in commercial scale DSSCs.

In addition, the DSSCs modules are fabricated by connecting few millimeter wide strips type area devices in Z or W type interconnection [125, 127]. Figure 2.23 shows two possible layouts in which cells are connected in series and it has been demonstrated that both the layouts have their advantages and disadvantages.

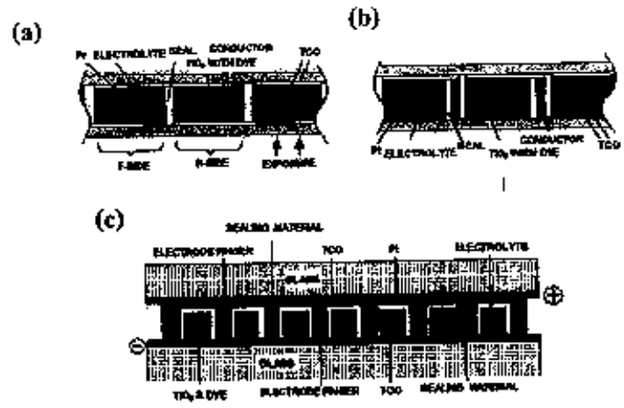

Figure 2.23 12-Cells connected in series in (a) W fashion, (b) Z fashion, and (c) cells connected in parallel [125].

The series interconnect modules are prepared by connecting individual small cells in series. Since each unit cell is prepared under ideal conditions, it is to be expected that the performance will be the same as that of the unit cell. Yi-Duo Zhang and colleague reported the optimized geometry of DSSCs module, which are mainly influenced by the manufacturing technique rather than the performance of the small cell [124]. Simulation shows that the large area DSSCs module with aperture area efficiency of 10.57% can be produced based on the small cell with efficiency of 11.1%. The module and division of a cell was shown in Figure 2.24. The module consisted of several sub-modules, which were series connected (Z-type) along direction x (only two sub-modules were shown in Figure. 2.24). Each sub-module consisted of several rectangular cells, which were connected in parallel along direction y. The active area of each cell had length L_X and width L_Y. Each cell was circled by silver fingers. The width of the silver finger between neighboring cells was W_S, and the width of the silver finger at the edge of

each sub-module was $W_S/2$. The distance between the active area and the silver finger was d_S. The distance between the neighboring sub-modules was d_m (extra space for series connection).

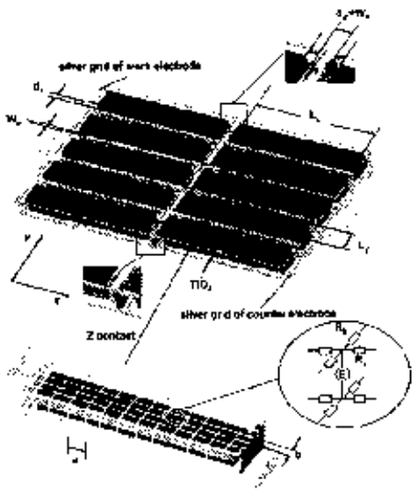

Figure 2.24 Sketch of a module and division of a cell. Each cell was divided into many rectangular sub cells. Each sub cell inactive area was simulated as eight resistances and one source [124].

Then, with the durability of the large size modules, some reports were published [130-133]. Hinsch et al. [131] reported that after 900 h ageing at 85°C with 4 cm^2 x 5 cells, a decrease of 30% in maximum power was observed. Shuji Nada and co-worker reported the DSSCs module of 120 mm^2 which has high temperature durability [130]. The durability was tested under 85°C for 100 h, at the end of the test the conversion efficiency was retained over 95% of the initial one. Figure 2.25 was shown the image of 120 mm^2 sub-module and 225 mm^2 module.

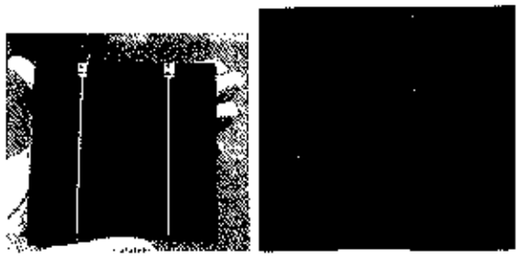

(a) **(b)**

Figure 2.25 The image of (a) 120 mm^2 sub-module and (b) 255 mm^2 module [130].

The 255 mm^2 module has 6-unit sub-modules on the FTO glass (255 mm ×255 mm × 4 mm), each sub-module is series-connected and similar to the 120 mm^2 sub-module, therefore the module is fabricated using nearly the same method of the 120 mm^2 sub-module.